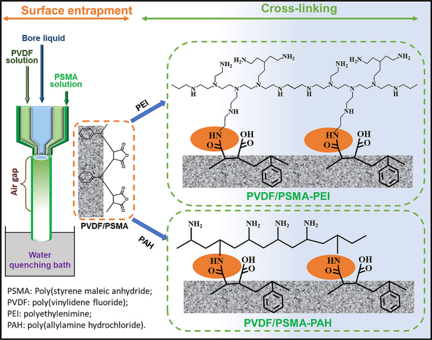
Surface entrapment
Cross-linking
Bore liquid
PVDF solution
PSMA solution
Air gap
Water quenching bath
PEI
PAH
PVDF/PSMA
PVDF/PSMA-PEI
PVDF/PSMA-PAH
PSMA: Poly(styrene maleic anhydride;
PVDF: poly(vinylidene fluoride);
PEI: polyethylenimine;
PAH: poly(allylamine hydrochloride).

Development of loose nanofiltration PVDF hollow fiber membrane for dye/salt separation

Pengfei Zhang [a,b], Saeid Rajabzadeh [a,b,c], Qiangqiang Song [a,b], Ralph Rolly Gonzales [a], Yuandong Jia [a,b], Shang Xiang [a,b], Zhan Li [a], Hideto Matsuyama [a,b]*

[a] *Research Center for Membrane and Film Technology, Kobe University, 1-1 Rokkodaicho, Nada, Kobe 657-8501, Japan*

[b] *Department of Chemical Science and Engineering, Kobe University, 1-1 Rokkodaicho, Nada, Kobe, 657-8501, Japan*

[c] *School of Civil and Environmental Engineering, University of Technology Sydney (UTS), City Campus, Broadway, NSW 2007, Australia*

** Corresponding author: Professor H. Matsuyama*

E-mail address: matuyama@kobe-u.ac.jp (H. Matsuyama)

Tel. / Fax: +81 78 803 6180

Abstract: The fabrication of loose nanofiltration (LNF) membranes for effective separation of dye/salt wastewater mixtures remains a great challenge. In this study, a new method for preparing a LNF membrane is proposed by combining co-extrusion technology and chemical cross-linking. Poly(styrene maleic anhydride (PSMA), an amphipathic copolymer was first entrapped onto the outer surface of poly(vinylidene fluoride) (PVDF) hollow fiber membranes (HFMs) by spinning using a triple orifice spinneret. Subsequently, the prepared PVDF/PSMA membranes were cross-linked using polyethylenimine (PEI) or poly(allylamine hydrochloride) (PAH). Finally, the chemical structure, morphology, hydrophilicity, zeta potential, and pore size were studied systematically. The small pore size and strong positive charge of the prepared membranes contributed to the high rejection of various dyes (> 99%) and low salt rejection (< 8.5%). The prepared membranes also exhibited excellent stability during long-term filtration. Antifouling experiments demonstrated that the prepared LNF membrane had good fouling reduction properties against bovine serum albumin (BSA) and lysozyme (LYZ). This study provides new perspectives for the design of useful LNF HFMs for the treatment of dye/salt wastewater mixtures.

Keywords: Loose nanofiltration, Hollow fiber membrane, Co-extrusion technology, Poly(vinylidene fluoride), Chemical cross-linking.

1. Introduction

Synthetic dyes are extensively used in paper, plastic, rubber, and textile manufacturing, generating a large amount of dye wastewater [1-5]. The indiscriminate disposal of wastewater from dyeing processes without appropriate treatment not only wastes a large number of resources, but also causes serious threat to aquatic ecosystems and human health. In addition, it is known that many salts produced in both dye production and dyeing processes are also present in dye wastewater, which makes the biodegradation of dye wastewater treatment more difficult [6-9]. Conventional wastewater treatment systems, i.e., coagulation, adsorption, photocatalysis, and chemical oxidation, have low efficiency for dye and salt mixture separation, and it is difficult to meet increasing regulatory requirements. With the development of membrane-based separation technologies, loose nanofiltration (LNF) membranes have become the most promising candidates for separating dyes and salts owing to their high dye retention and very low salt rejection, thus attracting much attention in recent years [3, 10, 11].

Compared to traditional nanofiltration (NF) membranes, LNF membranes are preferable for the separation of dye/salt mixed wastewater because of their significant rejection of dye molecules and high leakage of inorganic salts [2]. Various methods, including, surface coating, phase separation, interfacial polymerization (IP), and surface grafting, have been employed to fabricate high-performance LNF membranes [3, 6, 9, 12]. However, these methods still face difficulties that limit their industrial applications. For example, although interfacial polymerization has been established as a NF membrane fabrication method, the rapid and stochastic IP process makes it difficult to accurately control the pore size because the formation of a dense PA layer tends to reject multivalent salts, which is not appropriate for the fabrication of membranes to separate dye/salt wastewater. In addition, most of the methods mentioned above are restricted to flat sheet membranes, which means that their application to hollow fiber membranes (HFMs) is sometimes difficult; nevertheless, it is well known that HFMs possess the advantages of self-support, back-washability, and high packing density [13-16].

Among the aforementioned technologies, cross-linking is a common method for fabricating LNF membranes and has received broad public attention. Recently, the amphiphilic copolymer poly(styrene maleic anhydride) (PSMA) has been frequently employed for functional polymeric membrane preparation, followed by further cross-linking to obtain LNF membranes. For example, Jin et al. [11] first incorporated PSMA into a dope solution to prepare a polyether sulfone (PES)/PSMA-based membrane using non-solvent induced phase separation (NIPS) and surface grafting of polyethylenimine (PEI) via a cross-linking reaction, which resulted in a rejection rate of 99.4% for Congo red and 2.5% for NaCl, with high stability in the test run. Using the thermally induced phase separation (TIPS) process, Bian et al. [9] blended PSMA into a poly(vinylidene fluoride) (PVDF) polymeric solution to deposit a PSMA layer on the outer surface of HFMs. Following chemical crosslinking and metal ion coordination, a series of LNF membranes with high selectivity was prepared for separating various dyes (96.1% Crystal violet, 99.3% Sunset Yellow, and 99.5% Acid Red 27), as well as good stability during long-term operation. The presence of copolymer PSMA in the polymer dope solution, however, significantly influences the phase separation process, leading to negative effects on the membrane structure during membrane preparation [11, 17, 18]. More importantly, the incorporation of PSMA into the membrane bulk structure substantially reduces the mechanical properties of the membrane owing to its rigidity. This would be detrimental to the self-supporting process of HFMs.

Previously, our research group proposed a co-extrusion method utilizing a triple orifice spinneret (TOS) to tightly entrap polystyrene-based copolymer materials onto the outer surface of PVDF HFMs during the membrane fabrication process, in which the copolymer solution was extruded at the outermost layer of the TOS [19, 20]. The advantage of this method is that it does not change the membrane bulk structure, retaining nearly all the properties of the HFMs, because entrapment of the copolymer only occurs at the outer surface of the membrane. Furthermore, these copolymers with polystyrene segments entrapped on the PVDF membrane's outer surface exhibit good stability because of hydrophobic-hydrophobic interaction and intricate entanglement between the polystyrene segments and PVDF molecules [21, 22]. Hence, it is anticipated that substrate PVDF HFMs with reactive groups at the membrane's outer surface could be fabricated by co-extrusion method, and then further chemical crosslinking can be implemented to fabricate LNF membranes with selective layers.

The size exclusion effect and Donnan exclusion effect are the two main factors dominating the rejection of dyes and various salts [3, 10]. Thus, controlling the pore size and endowing the surface with a charge are feasible methods to prepare LNF membranes. PEI and poly(allylamine hydrochloride) (PAH) are two types of water-soluble polymers carrying a large number of amino groups and have been used in many studies to treat membrane surfaces [23-26]. Fortunately, amino groups can react with anhydride groups under relatively moderate conditions using a simple procedure, as already proven in previously published studies [9, 11, 27, 28].

Considering above, in this work we report a simple strategy combining co-extrusion technology and chemical cross-linking to fabricate LNF HFMs for dye/salt separation. As illustrated in Fig. 1(a), the amphipathic copolymer PSMA was firstly embedded onto the PVDF outer surface of the HFMs by extrusion at the outermost layer of the TOS to obtain a PVDF/PSMA substrate membrane. The amphiphilic copolymer PSMA consists of a large number of hydrophobic polystyrene and anhydride groups. Polystyrene groups can anchor into a polymeric matrix or become entangled with polymer molecules supporting good stability and avoiding detachment, whereas anhydride groups can conveniently serve as a functional group by reacting with amino groups or hydroxyl groups via a ring-opening reaction [17]. Then, PVDF/PSMA membrane was further cross-linked with PEI or PAH to obtain LNFs with a positively charged outer surface (Fig.1(c)). The morphologies, pore sizes, separation performance, long-term stability, and anti-fouling properties of the prepared membranes were systematically investigated. This work may expand into a new approach for the design and preparation of LNF HFMs to effectively separate dyes/salts wastewater based on co-extrusion technology in the membrane preparation process.

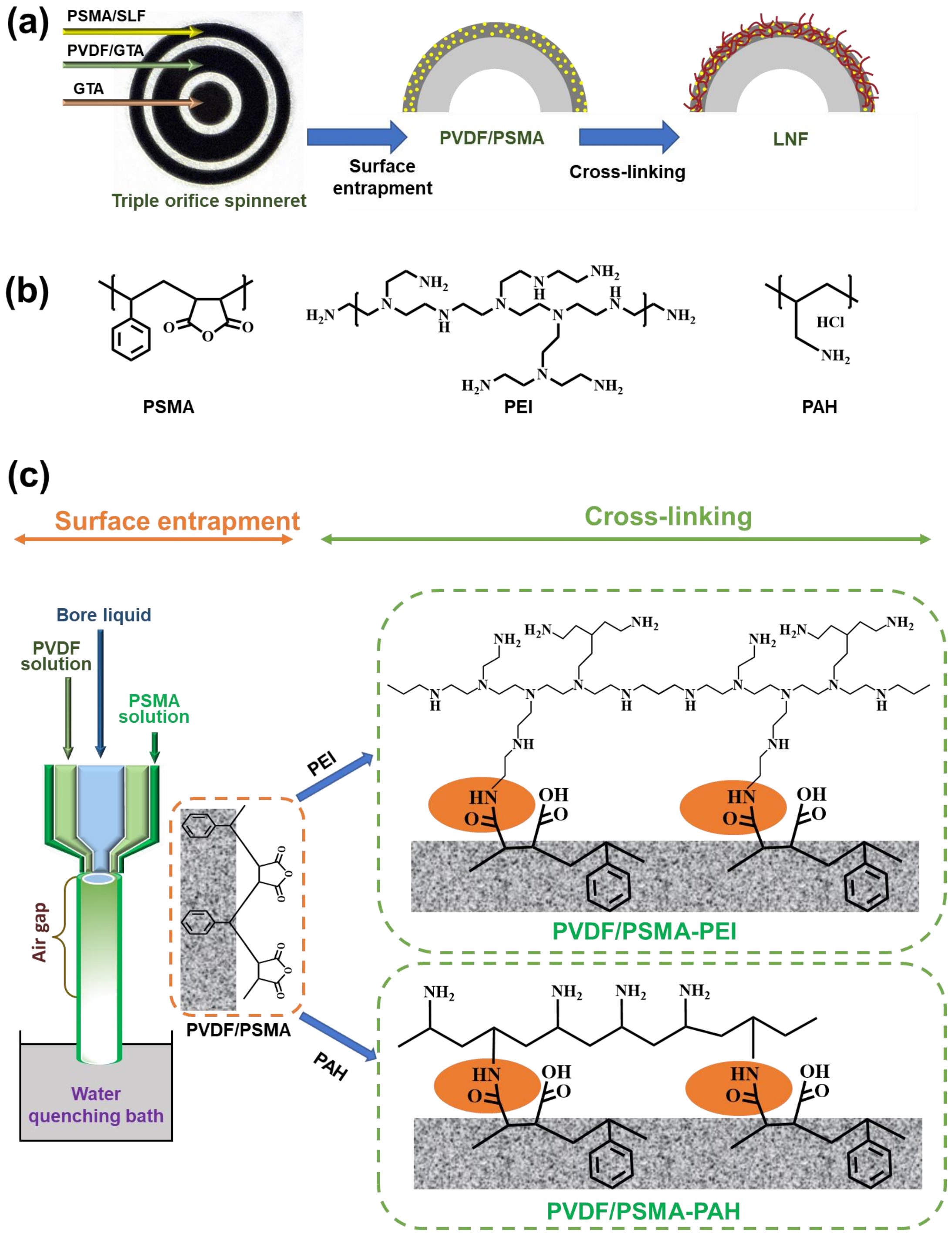

Fig. 1. Schematic of LNF membrane preparation process in this work (a), Chemical structure of PSMA, PEI, and PAH (b), Schematic of cross-linking between PSMA and PEI or PAH (c).

2. Experimental

2.1 Materials

PVDF powder (Solvay 6020, 687 kDa) was supplied by Solvay Specialty Polymers Japan (Tokyo, Japan). Random PSMA copolymers (XIRAN® 6000, polystyrene: anhydride = 6:1; M_W:10 kDa, powder) were provided by ORBISCOPE, powered by Polyscope Polymers (CZ Geleen, Netherlands). PEI solution (M_W:750 kDa, 50 wt% in H_2O) was purchased from Sigma-Aldrich (Japan). The PAH solution (M_W:100 kDa, 40 wt% in H_2O) was purchased from NITTOBO MEDICAL Co. (Tokyo, Japan). Congo red (CR) and Methyl blue (MB) dyes were purchased from Sigma-Aldrich (Japan), and Janus green B (JGB) and Erythrosine B (EB)was purchased from Tokyo Chemical Industry Co. (Tokyo, Japan). Sodium sulfate (Na_2SO_4, 99%), magnesium chloride ($MgCl_2$, 99%), triethylamine (TEA), potassium dihydrogen phosphate (KH_2PO_4), disodium phosphate (Na_2HPO_4), glycerol triacetate (GTA), sulfolane (SFL), ethanol, polyethylene glycol (PEG 1000, 2000, 4000, 6000, 8000, and 12000), bovine serum albumin (BSA), and lysozyme (LYZ) purchased from FUJIFILM Wako Pure Chemical Industries (Osaka, Japan). A Millipore Milli-Q unit was used to prepare purified water used in the experiments. All chemicals were used as received and without additional treatment.

2.2 Preparation of PVDF/PSMA-based HFMs

PVDF/PSMA HFMs were fabricated with a triple-orifice spinneret via the TIPS method, using a loop-type twin-screw extruder (TW05, ULTnano, Japan), as described previously [20]. GTA was selected as both diluent and bore liquid. SFL was used as the solvent for PSMA and was extruded at the outermost layer of the triple orifice spinneret. During membrane preparation, the PSMA/SFL, PVDF/GTA, and pure GTA were respectively extruded through the outer, middle, and inner layers of the triple orifice spinneret at the same time to form nascent membranes. They then successively passed through the air gap and water quenching bath and were collected using a take-up winder. The GTA was removed from the prepared membrane by immersion in ethanol. All parameters related to HFM preparation are shown in Table S1. The prepared HFMs (PVDF/PSMA) were stored in Milli-Q water.

2.3 LNF membrane preparation

The as-prepared PVDF/PSMA membranes were chemically cross-linked with PEI or PAH. The cross-linking is illustrated in Fig. 1(c). Before cross-linking, PVDF/PSMA substrate membranes with a length of 30 cm were rinsed with ethanol and Milli-Q water several times to completely remove the residual solvent. Then, they were subsequently immersed in aqueous PEI (or PAH) solution (2 wt%) prepared in advance, and whose pH was adjusted to 10.4–10.7. After adding TEA as a catalyst (0.25 wt%), the membranes were placed in an oven at 60 °C for 12 h to allow cross-linking to occur. Finally, all membranes were thoroughly rinsed with Milli-Q water to wash off unreacted PEI or PAH. Before the tests, the obtained LNF membranes were stored in Milli-Q water. The membranes cross-linked with PEI and PAH were designated PVDF/PSMA-PEI and PVDF/PSMA-PAH, respectively.

2.4 Membrane characterization

Attenuated total-reflectance Fourier-transform infrared (ATR-FTIR, Alpha Bruker) and X-ray photoelectron spectroscopy (XPS, JSP-9010MC, JEOL, Japan) were employed to determine the chemical composition of themembrane outer surface. Field-emission scanning electron microscopy (FE-SEM; JSF-7500F, JEOL, Japan) was used to examine the outer membrane surface and cross-sectional structure. Membrane hydrophilicity was evaluated using water contact angles (WCAs) were measured using a contact angle goniometer (Drop Master, Kyowa Interface Science Co., Japan). Liquid-liquid porometer (LLP-1100A, Porous Material Inc.) measured the pore size of the PVDF/PSMA membranes. The molecular weight cut-off (MWCO) and pore size distribution of PVDF/PSMA-PEI and PVDF/PSMA-PAH were obtained by the rejection rate of polyethylene glycols (PEGs) at various molecular weight of 1000, 2000, 4000, 6000, 8000, and 12,000 Da and a concentration of 1 g/L at an applied pressure of 1 bar. The feed and permeate solution concentrations were detected by a total organic carbon (TOC) meter (TOC-VCPH, SHIMADZU, Japan). The mean effective pore diameter (μ_p) was obtained as the Stokes diameter (d_s) of PEG showing 50% rejection. The Stokes diameter of PEG can be calculated using Eq. (1).

$$d_s = 33.46 \times 10^{-12} \times M_{PEG}^{0.557} \quad (1)$$

The pore size distribution was evaluated by mathematically fitting an exponential probability density function Eq. (2) [29-31]:

$$\frac{dR(d_P)}{dd_P} = \frac{1}{d_P \ln\sigma_P \sqrt{2\pi}} exp\left[-\frac{(\ln d_P - \ln\sigma\mu_P)^2}{2(\ln\sigma_P)^2}\right] \quad (2)$$

where μ_p is the mean effective pore diameter, and σ_p is the geometric standard deviation, which is the ratio of the pore diameters when R = 84.13% and 50%, d_p is the pore diameter.

2.5 Pure water permeability and rejection

Cross-flow filtration tests were conducted using a bench-scale setup with a laboratory-made hollow fiber filtration module [32]. The module contains a single hollow fiber membrane as illustrated in Fig. S1 with a length of 12 cm, resulting in an effective surface area of 7.5 cm^2. Prior to filtration, the membranes were first immersed in an ethanol solution until sufficiently wet. The feed solution was fed from the outside of the membrane to the inside using a peristaltic pump at a flow rate of 20 mL min^{-1} under a pressure of 1 bar. All the HFM modules were pre-compacted with DI water (1.5 bar) for 1 h prior to the permeation tests. Pure water permeance (PWP) (L m^{-2} h^{-1} bar^{-1}) is the average values of three modules, calculated using Eq. (3):

$$PWP = \frac{V}{At\Delta P} \quad (3)$$

where V is the volume (L) of the permeance at time t (h), A is the effective membrane area of the module tested (m^2), and ΔP is the applied transmembrane pressure (bar).

After the filtration of pure water, the feed solution was replaced with different aqueous 0.1 g L^{-1} dye solutions and 1 g L^{-1} salt solution to evaluate the selectivity of the membranes. The pH of all dye aqueous solution was adjusted at 7.0 and the dye concentration was detected using a U-200 UV spectrophotometer (Hitachi, Japan) at different wavelengths, as listed in Table S2, and the salt concentration was measured using a conductivity meter (Ultrameter IITM 4P, Myron L Company, Japan). The rejection (R) of the membranes was calculated using Eq. (4):

$$R = \left(1 - \frac{C_\mathrm{p}}{C_\mathrm{f}}\right) \times 100\% \quad (4)$$

where C_f and C_p are the concentrations of the dye and salt in the feed and permeate solutions, respectively.

2.6 Dynamic fouling filtration

The antifouling properties of the LNF membranes were assessed using a cyclic membrane fouling-rinsing procedure based on representative foulants with a concentration of 1 g L^{-1} (BSA and LYZ) under the same operating parameters as the separation performance evaluation [33]. The pH of the feed solution was fixed at 7.0 using a phosphate buffered saline solution. The evaluation process consisted of one cycle as follows: (1) pure water filtration for 1 h to determine the pure water flux (J_w1), (2) foulant solution filtration for 3 h to determine the fouling permeate flux (J_w2), (3) pure water was fed from the permeate channel (inside) to the feed channel for 1 h at 0.5 bar for backwashing as shown in Fig. S2, and (4) pure water filtration after backwashing for 1 h to determine (J_w3). For comparison, normalized flux is employed in this section, which is the ratio of the flux during the fouling experiment to the original water flux. Antifouling indices, such as flux recovery ratio (FRR), total fouling ratio (R_t), reversible fouling ratio (R_r), and irreversible fouling ratio (R_ir), were calculated to estimate the antifouling ability of the LNF membranes [34], as follows:

$$FRR = \frac{J_{w3}}{J_{w1}} \times 100\% \quad (5)$$

$$R_\mathrm{t} = 1 - \frac{J_{w2}}{J_{w1}} \times 100\% \quad (6)$$

$$R_\mathrm{r} = 1 - \frac{J_{w3} - J_{w2}}{J_{w1}} \times 100\% \quad (7)$$

$$R_\mathrm{ir} = 1 - \frac{J_{w3}}{J_{w1}} \times 100\% \quad (8)$$

2.7 Long-term filtration test

Long-term stability tests were conducted wherein dye/salt aqueous mixture solution (0.1 g L^{-1} CR and 1.0 g L^{-1} Na_2SO_4) were used as the feed solution for the PVDF/PSMA-PEI and PVDF/PSMA-PAH membranes. Filtration was performed at an applied pressure of 1 bar for 5 days. The permeation flux (J) and solute rejection rate (R) were determined as described above.

3. Results and discussion

3.1. Characterization of the HFMs

The ATR-FTIR spectra of the PVDF/PSMA, PVDF/PSMA-PEI, and PVDF/PSMA-PAH membranes are shown in Fig. 2(a). For both the PAH- and PEI-cross-linked membranes in comparison to the PVDF/PSMA, characteristic peaks belonging to the anhydride group (1779 and 1858 cm^{-1}) disappear, and three new peaks at 1558, 1645, and 3402 cm^{-1} are observed. These three new peaks are attributed to the N–H stretching band, C=O stretching band in amide groups, and the N–H stretching vibration [28, 35, 36], respectively, confirming a successful reaction between the anhydride and amine groups in both PAH and PEI.

Furthermore, the XPS spectra and surface element analysis of the resultant membranes are shown in Fig. 2(b) and Table 1, and the high-resolution spectra are shown in Figs. 2(c–f). As shown in Fig. 2(b), compared with the PVDF/PSMA membrane, the PVDF/PSMA-PEI and PVDF/PSMA-PAH membranes display a new peak at 400 eV assigned to the N element with contents of 7.69 and 6.94 at%, respectively (Table 1). Meanwhile, the intensity of the peak at 700 eV assigned to the F element significantly decreases from 25.8 at% to 5.16–6.07 at% as listed in Table 1, indicating PEI or PAH on the PVDF membrane outer surface. To determine the chemical reaction between PSMA and PEI or PAH, further analysis by narrow scanning of the C 1s spectra for all prepared membranes was carried out, as shown in Fig. 2(c). Figs. 2(d–f) show deconvoluted C 1s spectra of the PVDF/PSMA, PVDF/PSMA-PEI, and PVDF/PSMA-PAH membranes, respectively. The C 1s spectrum of the

PVDF/PSMA (Fig. 2(d)) was deconvoluted into five peaks with binding energies of 284.6, 285.7, 286.5, 288.4, and 291.0 eV which were assigned to C–H, C–H_2, C–O, O–C=O, and C–F, respectively. The dominance of the C–O and O–C=O from the anhydride groups. Combining the EDX result shown in Fig. S3, it was can be found that the copolymer PSMA is entrapped onto the membrane's outer surface. After cross-linking, two peaks at binding energies of 285.7 and 278.6 eV representing C–N and N–C=O are displayed for both PVDF/PSMA-PEI and PVDF/PSMA-PAH membranes confirming the reaction between anhydride and amine groups. Moreover, the relative intensity of the C–F peak is greatly weakened after cross-linking compared to that of the PVDF/PSMA membrane. These results confirm that the membrane surface is dominated by cross-linked PEI or PAH.

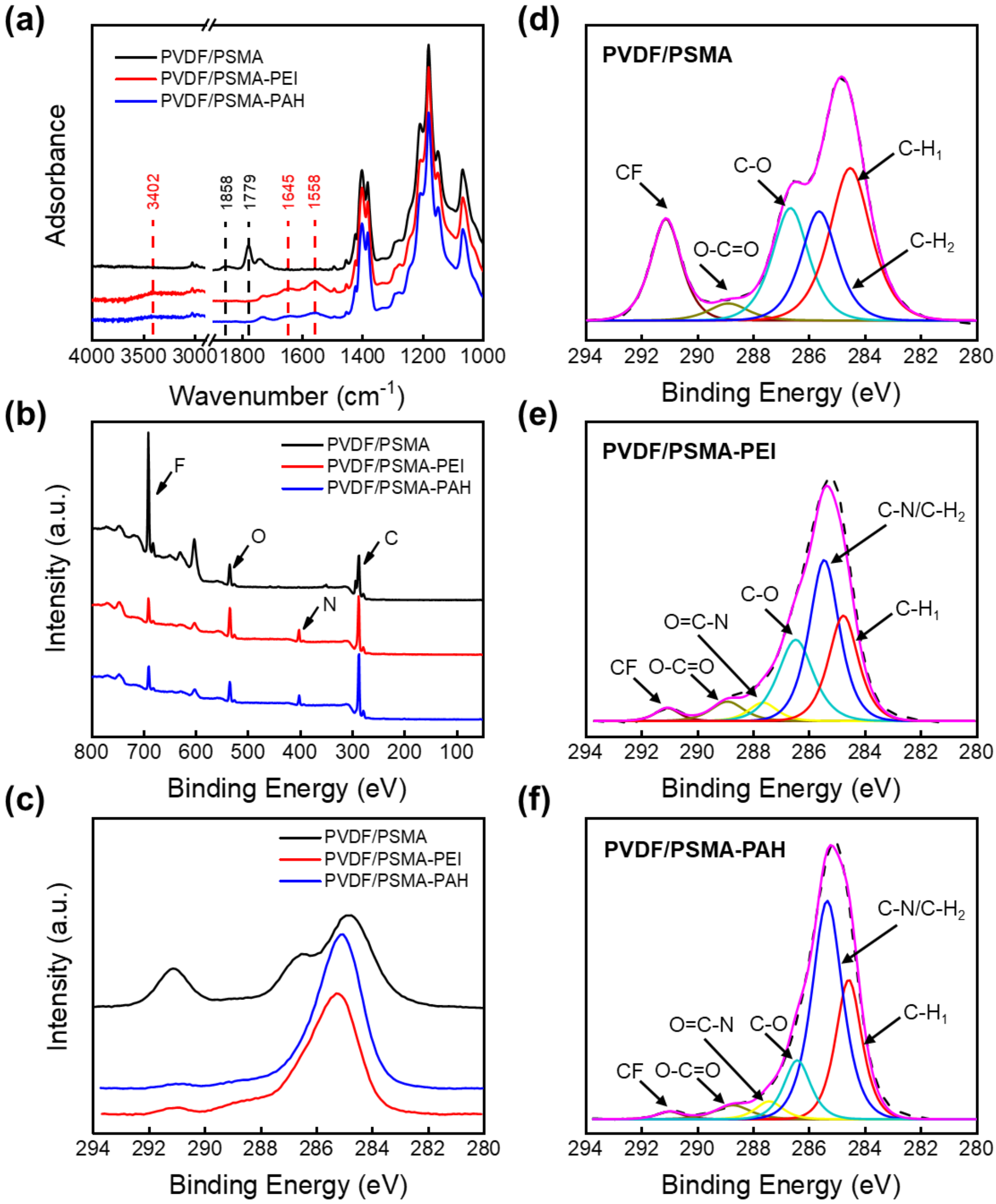

Fig. 2 ATR-FTIR spectra (a), XPS survey scan, (b), C 1s spectra of the prepared membranes (c), C 1s spectra for PVDF/PSMA, PVDF/PSMA-PEI, and PVDF/PSMA-PAH membranes (d-f), respectively.

Table 1 Membrane elemental composition measured by XPS.

Membrane	**C**	**F**	**O**	**N**
PVDF/PSMA	66.3	25.8	7.86	0
PVDF/PSMA-PEI	75.0	5.16	12.2	7.64
PVDF/PSMA-PAH	78.2	6.07	8.78	6.94

The cross-sectional and outer surface structures of the resultant membranes were investigated using FE-SEM as shown in Fig. 3. From cross-sectional images, the substrate PVDF/PSMA membrane shows loose and porous structure in the cross section near the outer surface (Fig. 3(d)). After the cross-linking, both PEI and PAH based LNF membranes take on a relative dense thin skin layer near the outer surface (Fig. 3(e) and (f)). Accordingly, the PVDF/PSMA membrane also exhibits a porous outer surface (Fig. 3(g)). the porous structure disappears, and a denser layer with substantially larger ridges is generated at the outer surface of the PVDF/PSMA-PEI membrane (Fig. 3(h) and (i)). This is because the cross-linking layer constructed with PEI is sufficiently dense to overlap the substrate surface entirely. Notably, the crosslinking reaction between PSMA and PEI becomes more pronounced, resulting in the formation of numerous aggregate nodules on the outer surface. This is in accordance with the literature [37]. As for the PVDF/PSMA-PAH membrane, almost the same morphology as that of the PVDF/PSMA-PEI membrane is formed at the outer surface owing to the cross-linking reaction.

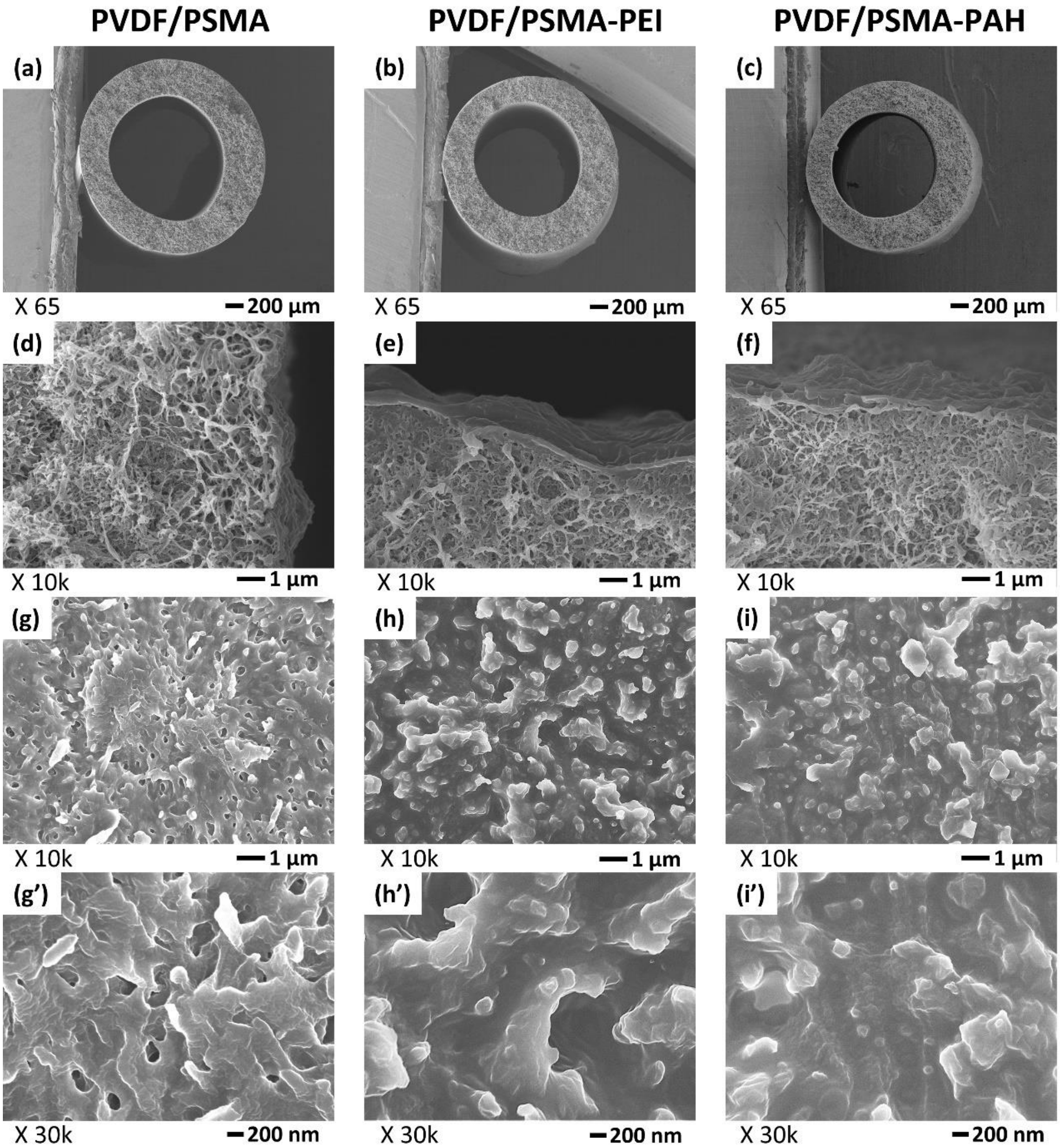

Fig. 3 FE-SEM images of the prepared membranes: PVDF/PSMA, PVDF/PSMA-PEI, and PVDF/PSMA-PAH. Cross section (a) - (c); cross section near the outer surface (d) - (f); outer surface (g) - (i); and high magnification images of the outer surface (g') - (i').

The water contact angle (WCA) was measured to evaluate the hydrophilicity of the membrane surfaces, and the results are presented in Fig. 4(a). The WCA of the PVDF membrane outer surface entrapped by the amphipathic copolymer PSMA is approximately 92°, indicating a hydrophobic outer surface. In comparison to the PVDF/PSMA membrane, an obvious decline in WCA is observed for both the

PVDF/PSMA-PEI and PVDF/PSMA-PAH membranes, dropping to 68° and 73°, respectively. Because PEI and PAH are hydrophilic, the membrane surface hydrophilicity is strengthened by the coverage with PEI or PAH.

The outer surface charge of the PEI- and PAH-crosslinked membranes was also investigated. As shown in Fig. 4(b), the PVDF/PSMA substrate has a negative charge above a pH value of 3.43, which is considered the isoelectric point (IEP). However, the PEI- and PAH-cross-linked membranes exhibit positive charges when the pH is lower than 9 and 10.32, respectively. This is because the $-NH_2$ groups in PEI and PAH molecules can combine with H^+ in an aqueous solution to form the ammonium group $-NH_3^+$, which results in a positively charged surface [38]. In addition, the membrane grafted by PAH has a higher positive zeta potential than that grafted by PEI in the pH range investigated, owing to the higher number of $-NH_2$ groups per gram of PAH molecule.

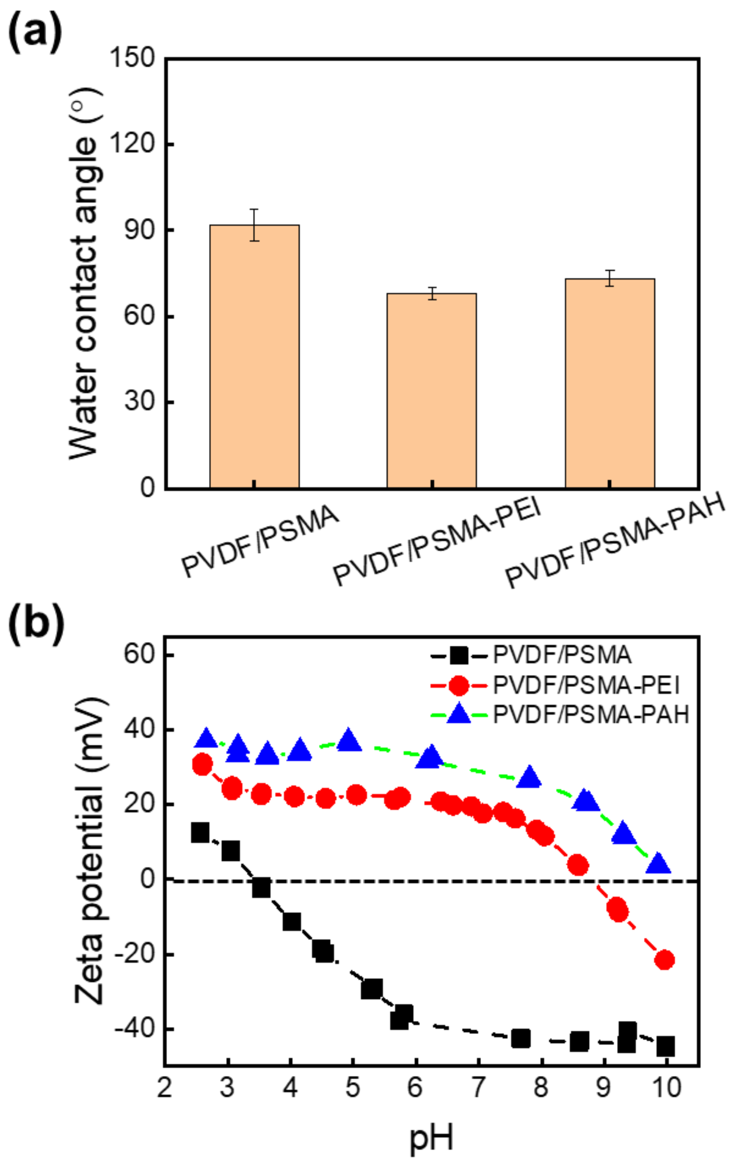

Fig. 4 Water contact angle (a) and Zeta potential (b) of the outer surface of prepared membranes.

Fig. 5(a) displays the pore size and pore size distribution of the PVDF/PSMA membrane determined using a liquid-liquid porometer. The PVDF/PSMA substrate exhibits a mean pore size of approximately 27.5 nm with a broad pore distribution. As for the cross-linked LNF membranes, the pore size was evaluated by the molecular weight cut-off (MWCO) tested with different molecular weights of polyethylene glycol (PEG), as shown in Fig. S4. The MWCO values of PVDF/PSMA-PEI and PVDF/PSMA-PAH were 7020 Da and 7480 Da, respectively. Both types of cross-linked membranes exhibit a narrower pore distribution (Fig. 5(b)) than that of the PVDF/PSMA membrane. These results confirm that successful LNF membranes can be prepared by combining a surface entrapment process with co-extrusion technology and the subsequent chemical cross-linking used in this work.

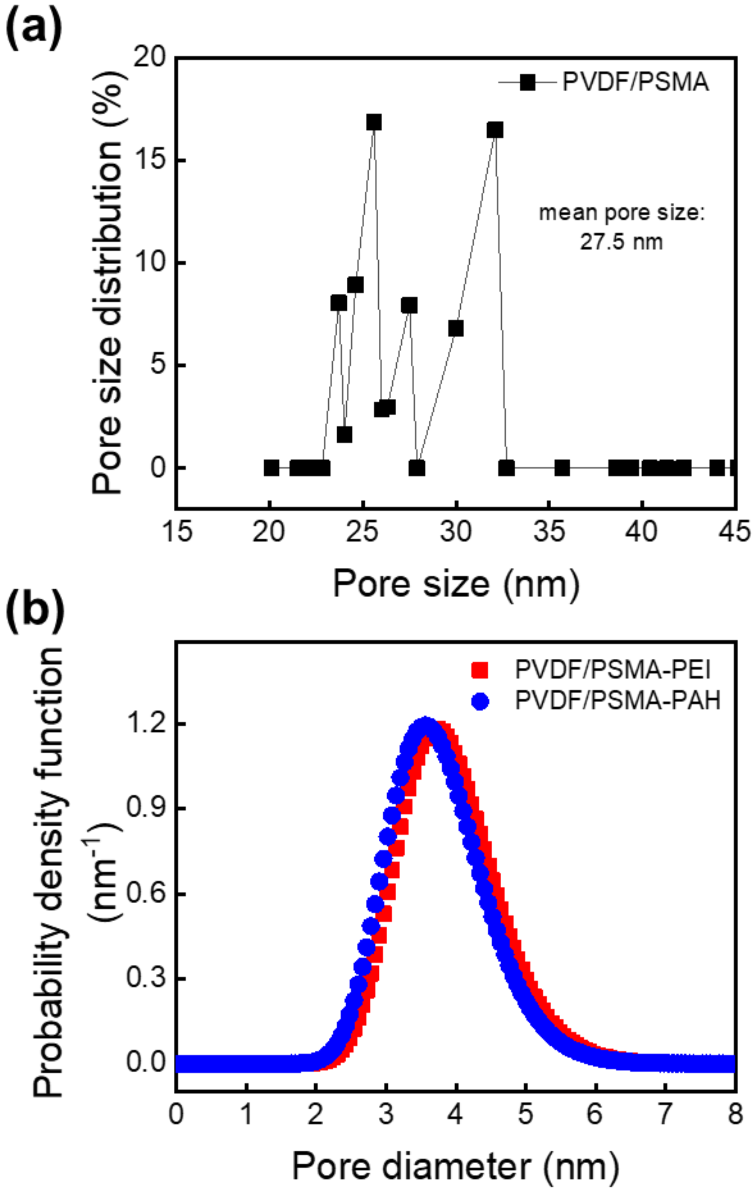

Fig. 5 Pore size and distribution of PVDF/PSMA membrane tested by liquid-liquid porometer (a) and of PVDF/PSMA-PEI and PVDF/PSMA-PAH calculated by PEG rejection (b).

3.2 Filtration performance

The separation performance of the prepared LNF membranes was systematically investigated to estimate their permeability and rejection of dyes and salts. It is generally known that pure water flux is proportional to applied pressure [39, 40]. Fig. 6(a) presents the influence of applied pressure on pure water flux of the resultant membranes. It can be seen that the pure water flux of all the membranes increases with an increase in operating pressure: 27.0, 60.0, and 81.9 L $m^{-2}h^{-1}$ for PVDF/PSMA, 9.5, 20.4, and 25.7 L $m^{-2}h^{-1}$ for PVDF/PSMA-PEI, and 8.6, 18.87, and 25.1 L $m^{-2}h^{-1}$ for PVDF/PSMA-PAH at applied pressures of 0.5, 1, and 1.5 bar, respectively. Comparing the water flux under a fixed pressure, the water flux of the cross-linked membranes dropped to almost one-third of that of the PVDF/PSMA membrane owing to the dense layer formed through chemical cross-linking.

Fig. 6(b) shows the rejection rate of the four dye solutions, as listed in Table S2. Methyl blue (MB) and Congo red (CR) are negatively charged dyes, while Janus Green B (JGB) is positively charged and Erythrosin B (EB) is neutral. As shown in Fig. 6(b), the PVDF/PSMA membrane has a low rejection rate (< 30%) for all dyes used. In particular, for the neutral dye EB, the rejection rate is almost zero. These low rejection rates can be explained by the large pore size, as shown in Fig. 5(a), which suggests that further modification is required. After cross-linking, the PVDF/PSMA-PEI membrane shows a rejection rate ≥ 99.3% for MB, CR, and EB, and 87.3% for positively charged JGB, whereas the PVDF/PSMA-PAH membrane exhibits a rejection rate of > 99.0% for all dyes. Neutral EB is completely rejected by these two membranes owing to size sieving. Notably, the rejection rate (99.8%) of the PVDF/PSMA-PAH membrane for the positively charged JGB with the smallest molecular weight is much higher than that of the PVDF/PSMA-PEI membrane (87.3%). The pore diameter of the PVDF/PSMA-PAH membrane is slightly smaller than that of the PVDF/PSMA-PEI membrane, as shown in Fig. 5(b). This rejection difference is ascribed to the synergistic effect of electrostatic repulsion and size sieving. As shown in Fig. 4(b), the PVDF/PSMA-PAH membrane has a stronger positive zeta potential (29.0 mV) than that of the PVDF/PSMA-PEI membrane (17.6 mV) at pH 7.0. This indicates that the electrostatic repulsion between the positive dye and positive membrane is more pronounced in the

PVDF/PSMA-PAH membrane. The smaller pore size of the PVDF/PSMA-PAH membrane also contributes to higher rejection by the size sieving effect. Furthermore, the water permeance of all the prepared membranes in the case of the CR feed solution (Fig. S5) is lower than that of pure water (Fig.6(a)), probably because of the osmotic pressure of the feed solution [8, 41].

The permeance and salt rejection ability of the resultant membranes were studied using Na_2SO_4 and $MgCl_2$ salts. Fig. 6(c) indicates that the $MgCl_2$ and Na_2SO_4 rejection rates of the PAH- and PEI-cross-linked membranes are sufficiently low (~8.5%) and almost identical. All the water permeance values for the salt solutions are lower than those for pure water permeance, owing to the osmotic pressure of the feed solution. The effect of Na_2SO_4 concentration on the filtration performance was investigated, as shown in Fig. 6(d). It can be seen that Na_2SO_4 concentration has no effect on the permeance and rejection for PVDF/PSMA substrate membrane, which results from its quite big pore size. The water permeance decreases with increasing Na_2SO_4 concentration, in accordance with the literature [8, 35]. This is because the higher osmotic pressure of the feed solution caused by the higher Na_2SO_4 concentration decreases the driving force for water permeation.

As described above, the two types of LNF membranes prepared in this study (PVDF/PSMA-PAH and PVDF/PSMA-PEI) show high dye rejection (>99%) and low solute rejection (~8.5%), indicating that these membranes are useful for the treatment of dye/salt wastewater.

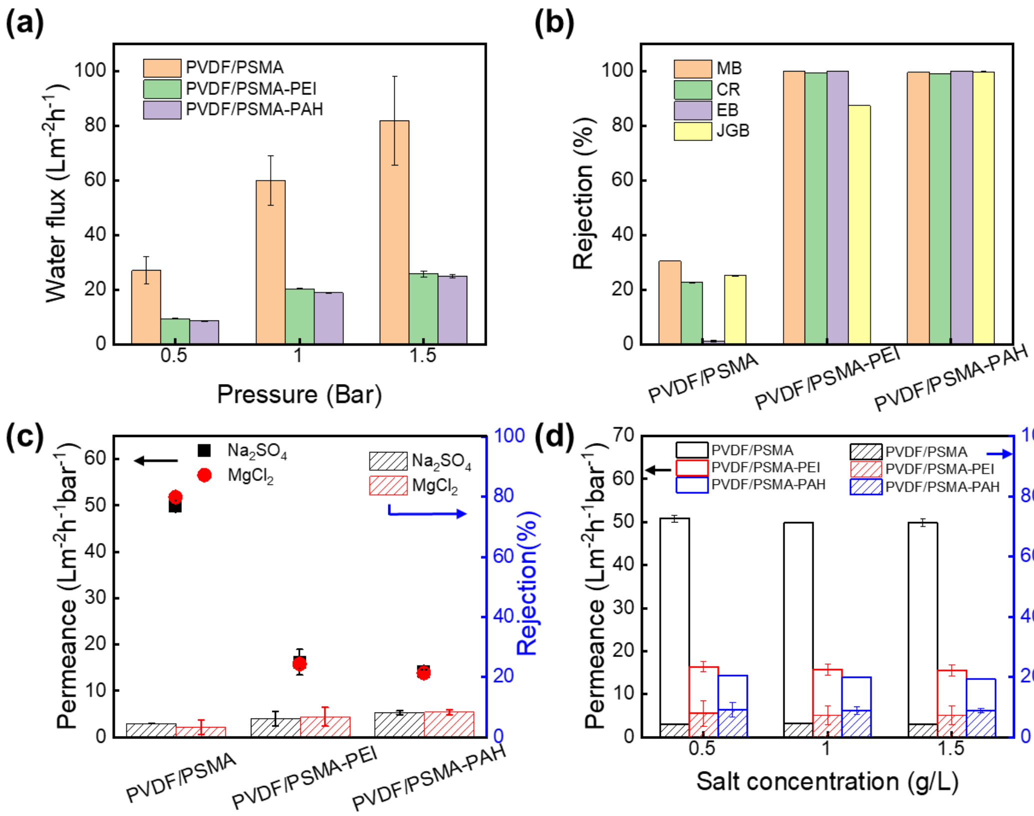

Fig. 6 Filtration performance of prepared membranes outer surface: Effect of operating pressure on water permeance (a), rejection rates of dyes operated at a pressure of 1 bar (b), salt rejection rate and permeance for feed Na_2SO_4 and $MgCl_2$ solutions operated at a pressure of 1 bar (c), and effect of Na_2SO_4 concentration on filtration performance operated at a pressure of 1 bar.

3.3. Antifouling performance

The overall separation performance of membranes is often plagued by membrane fouling, which significantly affects the life span of membranes. In this study, antifouling experiments were conducted on the prepared membranes. Two types of model foulants were selected for the evaluation of membrane fouling behavior: BSA and LYZ. BSA (IEP 4.7) was negatively charged, whereas LYZ (IEP 10.5, [42]) was positively charged because the feed solution pH was 7. The effects of the foulants on the water flux of the PVDF/PSMA, PVDF/PSM-PEI, and PVDF/PSMA-PAH membranes are presented in Fig. 7, and the detailed flux decline ratio after fouling and flux recovery ratio after backwashing are listed in Table 2. In the case of BSA, it is evident from Fig. 7(a) that the normalized flux of all the membranes sharply decreases after feeding the foulant solution and then becomes nearly constant. After back-washing and then feeding with pure water again, the water flux is recovered, but the degree of recovery is dependent on the membrane type. For BSA antifouling experiments, as shown in Table 2, the FRR values of PVDF/PSMA, PVDF/PSM-PEI, and PVDF/PSMA-PAH membranes are 41, 77, and 73%, respectively. It was expected that the PVDF/PSMA membrane would have a higher FRR value because its negatively charged surface would cause strong electrostatic repulsion toward the negatively charged BSA molecules. However, compared with the PVDF/PSMA membrane, the PVDF/PSM-PEI and PVDF/PSMA-PAH membranes with positive charges exhibit higher FRR values. Membrane fouling behavior is also strongly related to surface hydrophilicity [42]. For the PVDF/PSMA membrane with a relatively high water contact angle, hydrophobic interactions between the membrane surface and BSA cause severe adsorption [35]. Moreover, the BSA molecules can pass through the membrane pores and are blocked in the pores owing to the large pore size of the PVDF/PSMA membrane, as shown in Fig. 5(a). Although PEI and PAH impart a positive charge to the membrane surface, their enhanced hydrophilic nature and small pore formation improve fouling resistance [43], showing comparatively low flux decline, high flux recovery, and high reversible fouling ratio (R_r), as shown in Table 2. Owing its relatively high hydrophilicity shown in Fig. 4(a), PVDF/PSM-PEI demonstrated a slightly higher BSA fouling resistance than PVDF/PSMA-PAH.

In the case of positively charged LYZ, as shown in Fig. 7(b) and Table 2, both PVDF/PSM-PEI (84%) and PVDF/PSMA-PAH (92%) membranes show a significant enhancement in FRR values compared with the PVDF/PSMA membrane (31%) due to the strong electrostatic repulsion between membrane surface and foulant. Compared to PEI cross-linked membrane, PAH modified LNF exhibited a lower Rt and Rir value listed in Table 2 for LYZ because its stronger positive charge existing on membrane outer surface shown in Fig. 4(b). The FRR values for PEI and PAH modified membranes in LYZ are higher than those for BSA (77 and 73%). In addition, the total fouling ratios (R_t) of these two LNF membranes during the fouling experiment are approximately 41 and 33%, respectively, which are lower than those of BSA (56 and 53%). The suppressed flux decline and improved flux recovery in the case of LYZ are attributed to electrostatic repulsion between the positively charged foulant and positively charged membrane surface, in addition to the improved membrane hydrophilicity and pore size reduction.

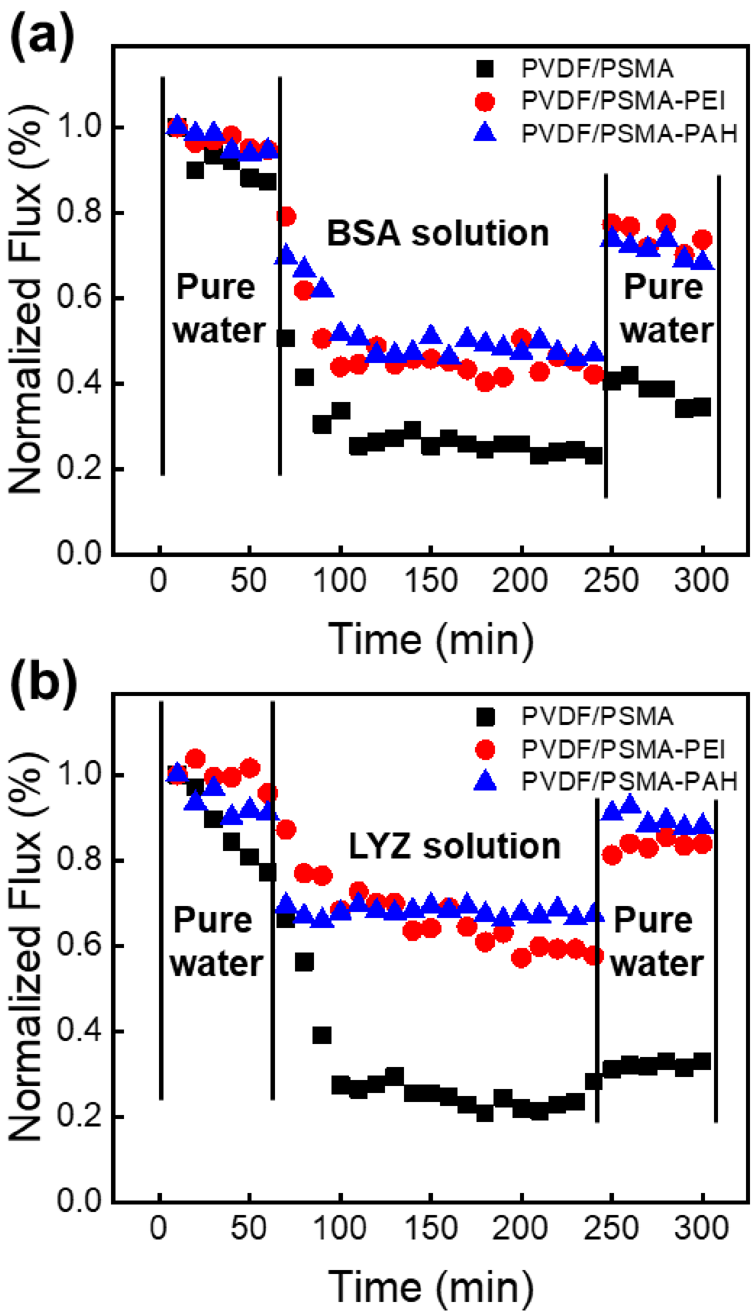

Fig. 7 Antifouling behavior of prepared membranes with the foulants BSA (a) and LYZ (b) under a pressure of 1 bar.

Table 2. Antifouling indexes of membranes for BSA and LYZ solution.

Membrane	BSA				LYZ			
	FRR	R_t	R_r	R_{ir}	FRR	R_t	R_r	R_{ir}
PVDF/PSMA	41	76	17	59	31	77	8	69
PVDF/PSMA-PEI	77	56	33	23	84	41	25	16
PVDF/PSMA-PAH	73	53	26	27	92	33	25	8

3.4. Long-term stability test for dye/salt separation

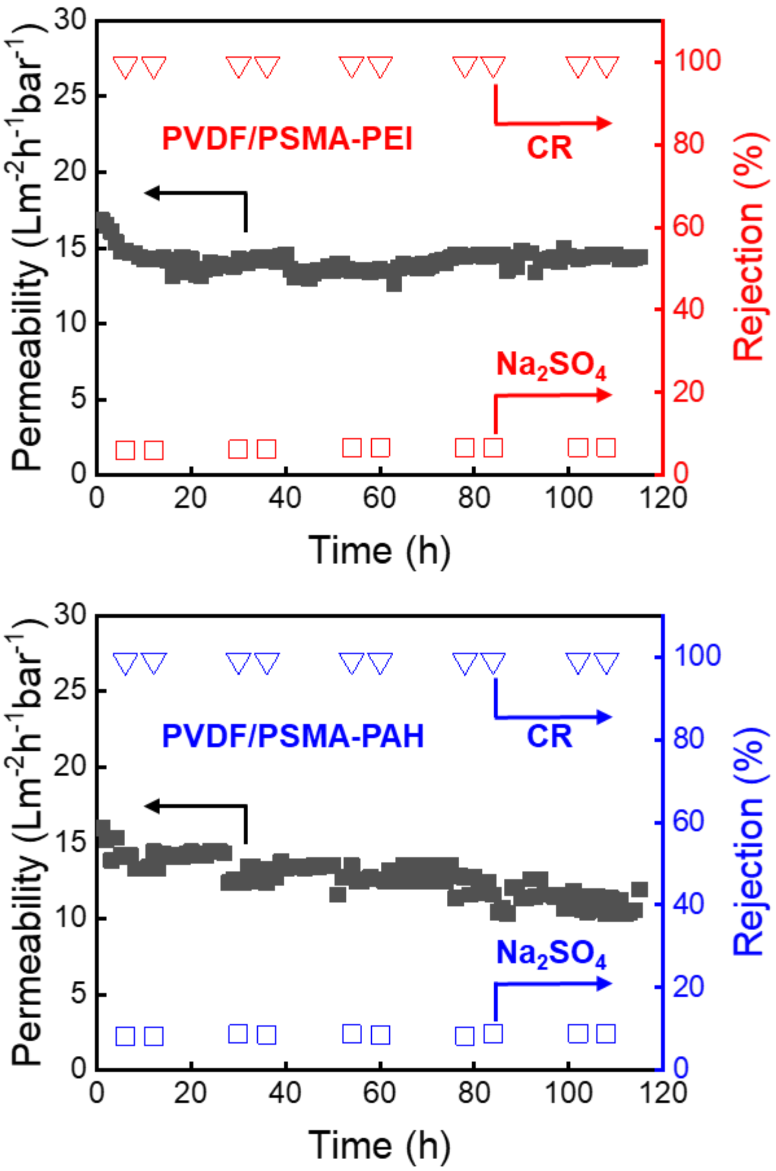

Fig. 8 Long-term filtration of prepared LNF membranes PVDF/PSMA-PEI (a) and PVDF/PSMA-PAH (b) with dye/salt mixture solution (CR/Na_2SO_4).

The long-term filtration by PVDF/PSM-PEI and PVDF/PSMA-PAH membranes was also investigated with a mixture of dye CR (0.1 g/L) and salt Na_2SO_4 (1 g/L) solution for 120 h, and the results are depicted in Fig. 8. It can be seen that the permeance of both tested membranes was almost constant for 120 h. It is important to note that both LNF membranes also show a high rejection rate for CR (> 99%) and a low rejection rate (8.0–9.0%) for Na_2SO_4 over the test period. These long-term stability tests demonstrate that the prepared LNF membranes have excellent performance stability in dye/salt wastewater, in terms of `permeance and dye/salt selectivity.

A comparison with other reported LNF hollow-fiber membranes is presented in Table 3. The LNF membranes prepared in this work by combining surface entrapment with co-extrusion technology and further chemical cross-linking demonstrate high performance for application in dye wastewater treatment.

Table 3. Comparisons of dye/salt separation performances of LNF hollow fiber membranes reported in the literature.

Membrane	PWP ($L\ m^{-2}h^{-1}bar^{-1}$)	Dye rejection (%)	Salt rejection (%)	Ref
PVDF	13.51	> 99.69	~ 6.3	[8]
PA/PVDF	10.2	99.4	32	[9]
PEI/CMCNa/PP	14.0	99.4	15.5	[44]
PES	~ 8.6	99.9	> 20	[15]
PSF/PES-COOH	228.9	98	~ 11	[16]
PVDF/GO	24.1	99.9	~ 11	[45]
PVDF/PSMA-PEI	20.4	99.4	6.1	This work
PVDF/PSMA-PAH	18.8	99.1	8.1	This work

PWP = Pure water permeance

Dye rejection: Congo red (CR) rejection.

Salt rejection: Na_2SO_4 rejection.

4. Conclusion

In summary, we developed a method to prepare loose nanofiltration membranes via a new method of surface entrapment of copolymers followed by chemical cross-linking. First, the outer surface of the PVDF HFMs was functionalized with the amphipathic copolymer PSMA using a triple-orifice spinneret during the preparation process. Then, two kinds of polymers with a high cation density, PEI and PAH, were employed for chemical cross-linking to form a selective dense layer, which lowered the pore size and imparted a strong positive charge on the outer surface of the membrane. The resultant membranes displayed high rejection of various dyes (99.1%) and low salt rejection (8.1%) with remarkable long-term stability. Moreover, the antifouling behavior of the developed positively charged LNF membrane was investigated with different types of foulants, including BSA and lysozyme. The prepared LNF membranes exhibit good anti-fouling properties. These results demonstrate a feasible method for producing LNF membranes for practical applications in dye wastewater treatment.

Conflicts of interest

There are no conflicts to declare.

Acknowledgements

Pengfei Zhang expresses his gratitude for the financial support provided by the China Scholarship Council (File No. 202008050076).

This work was partially supported by Kobe University Strategic International Collaborative Research Grant (Type B Fostering Joint Research)

References

[1] B. Van der Bruggen, E. Curcio, E. Drioli, Process intensification in the textile industry: the role of membrane technology, J. Environ. Manage., 73 (2004) 267-274.

[2] S. Guo, Y. Wan, X. Chen, J. Luo, Loose nanofiltration membrane custom-tailored for resource recovery, Chem. Eng. J., 409 (2021) 127376.

[3] X. Feng, D. Peng, J. Zhu, Y. Wang, Y. Zhang, Recent advances of loose nanofiltration membranes for dye/salt separation, Sep. Purif. Technol., 285 (2022) 120228.

[4] W.-J. Lau, A.F. Ismail, Polymeric nanofiltration membranes for textile dye wastewater treatment: Preparation, performance evaluation, transport modelling, and fouling control — a review, Desalination, 245 (2009) 321–348.

[5] A.K. An, J. Guo, S. Jeong, E.J. Lee, S.A.A. Tabatabai, T. Leiknes, High flux and antifouling properties of negatively charged membrane for dyeing wastewater treatment by membrane distillation, Water Res., 103 (2016) 362-371.

[6] C. Liu, H. Mao, J. Zheng, S. Zhang, In situ surface crosslinked tight ultrafiltration membrane prepared by one-step chemical reaction-involved phase inversion process between activated PAEK-COOH and PEI, J. Membr. Sci., 538 (2017) 58-67.

[7] Q. Li, Z. Liao, X. Fang, D. Wang, J. Xie, X. Sun, L. Wang, J. Li, Tannic acid-polyethyleneimine crosslinked loose nanofiltration membrane for dye/salt mixture separation, J. Membr. Sci., 584 (2019) 324-332.

[8] H. Liu, Y. Chen, K. Zhang, C. Wang, X. Hu, B. Cheng, Y. Zhang, Poly(vinylidene fluoride) hollow

fiber membrane for high-efficiency separation of dyes-salts, J. Membr. Sci., 578 (2019) 43-52.

[9] L. Bian, C. Shen, C. Song, S. Zhang, Z. Cui, F. Yan, B. He, J. Li, Compactness-tailored hollow fiber loose nanofiltration separation layers based on “chemical crosslinking and metal ion coordination” for selective dye separation, J. Membr. Sci., 620 (2021) 118948.

[10] J. Ding, H. Wu, P. Wu, Preparation of highly permeable loose nanofiltration membranes using sulfonated polyethylenimine for effective dye/salt fractionation, Chem. Eng. J., 396 (2020) 125199.

[11] J. Jin, X. Du, J. Yu, S. Qin, M. He, K. Zhang, G. Chen, High performance nanofiltration membrane based on SMA-PEI cross-linked coating for dye/salt separation, J. Membr. Sci., 611 (2020) 118307.

[12] M. Hu, S. Yang, X. Liu, R. Tao, Z. Cui, C. Matindi, W. Shi, R. Chu, X. Ma, K. Fang, M. Titus, B.B. Mamba, J. Li, Selective separation of dye and salt by PES/SPSf tight ultrafiltration membrane: Roles of size sieving and charge effect, Sep. Purif. Technol., 266 (2021) 118587.

[13] H. Roth, T. Luelf, A. Koppelmann, M. Abel, M. Wessling, Chemistry in a spinneret – Composite hollow fiber membranes in a single step process, J. Membr. Sci., 554 (2018) 48-58.

[14] N.T. Hassankiadeh, Z. Cui, J.H. Kim, D.W. Shin, S.Y. Lee, A. Sanguineti, V. Arcella, Y.M. Lee, E. Drioli, Microporous poly(vinylidene fluoride) hollow fiber membranes fabricated with PolarClean as water-soluble green diluent and additives, J. Membr. Sci., 479 (2015) 204-212.

[15] Z. Chu, K. Chen, C. Xiao, D. Ji, H. Ling, M. Li, H. Liu, Improving pressure durability and fractionation property via reinforced PES loose nanofiltration hollow fiber membranes for textile wastewater treatment, Journal of the Taiwan Institute of Chemical Engineers, 108 (2020) 71-81.

[16] D. Yao, F. Zhang, G. Feng, Y. Zhang, J. Meng, High-flux PSF/PES-COOH hollow fiber loose nanofiltration membrane for high-efficiency dye-salt separation, Journal of Environmental Chemical Engineering, 10 (2022) 108180.

[17] P. Zhang, S. Xiang, H. Wang, Y. Wang, J. Zhang, Z. Cui, J. Li, B. He, Understanding the multiple functions of styrene-co-maleic anhydride in fabricating polyvinylidene fluoride hollow fiber membrane via coupled phase inversion process and its effect on surface infiltration behavior and membrane permeability, J. Membr. Sci., 590 (2019) 117269.

[18] Z. Wu, Z. Cui, T. Li, S. Qin, B. He, N. Han, J. Li, Fabrication of PVDF-based blend membrane with a thin hydrophilic deposition layer and a network structure supporting layer via the thermally induced phase separation followed by non-solvent induced phase separation process, Appl. Surf. Sci., 419 (2017) 429-438.

[19] P. Zhang, S. Rajabzadeh, A. Venault, S. Wang, Q. Shen, Y. Jia, C. Fang, N. Kato, Y. Chang, H. Matsuyama, One-step entrapment of a PS-PEGMA amphiphilic copolymer on the outer surface of a hollow fiber membrane via TIPS process using triple-orifice spinneret, J. Membr. Sci., 638 (2021) 119712.

[20] P. Zhang, S. Rajabzadeh, T. Istirokhatun, Q. Shen, Y. Jia, X. Yao, A. Venault, Y. Chang, H. Matsuyama, A novel method to immobilize zwitterionic copolymers onto PVDF hollow fiber membrane surface to obtain antifouling membranes, J. Membr. Sci., 656 (2022) 120592.

[21] N.J. Lin, H.S. Yang, Y. Chang, K.L. Tung, W.H. Chen, H.W. Cheng, S.W. Hsiao, P. Aimar, K. Yamamoto, J.Y. Lai, Surface self-assembled PEGylation of fluoro-based PVDF membranes via hydrophobic-driven copolymer anchoring for ultra-stable biofouling resistance, Langmuir, 29 (2013) 10183-10193.

[22] A. Venault, M.R.B. Ballad, Y.-H. Liu, P. Aimar, Y. Chang, Hemocompatibility of PVDF/PS-b-PEGMA membranes prepared by LIPS process, J. Membr. Sci., 477 (2015) 101-114.

[23] S. Zhao, Z. Wang, A loose nano-filtration membrane prepared by coating HPAN UF membrane with

modified PEI for dye reuse and desalination, J. Membr. Sci., 524 (2017) 214-224.
[24] S. Rajabzadeh, C. Liu, L. Shi, R. Wang, Preparation of low-pressure water softening hollow fiber membranes by polyelectrolyte deposition with two bilayers, Desalination, 344 (2014) 64-70.
[25] Y. Jia, K. Guan, P. Zhang, Q. Shen, S. Wang, Y. Lin, H. Matsuyama, Surface engineering with microstructured gel networks for superwetting membranes, J. Mater. Chem., 9 (2021) 7924-7934.
[26] W.-Z. Qiu, Z.-S. Zhao, Y. Du, M.-X. Hu, Z.-K. Xu, Antimicrobial membrane surfaces via efficient polyethyleneimine immobilization and cationization, Appl. Surf. Sci., 426 (2017) 972-979.
[27] J.J. Lin, Y.C. Hsu, Temperature and pH-responsive properties of poly(styrene-co-maleic anhydride)-grafting poly(oxypropylene)-amines, J. Colloid Interface Sci., 336 (2009) 82-89.
[28] X. Duan, J. Xiao, Q. Yin, Z. Zhang, S. Mao, Y. Li, Amphiphilic graft copolymer based on poly(styrene-co-maleic anhydride) with low molecular weight polyethylenimine for efficient gene delivery, Int J Nanomedicine, 7 (2012) 4961-4972.
[29] Z. Thong, J. Gao, J.X.Z. Lim, K.-Y. Wang, T.-S. Chung, Fabrication of loose outer-selective nanofiltration (NF) polyethersulfone (PES) hollow fibers via single-step spinning process for dye removal, Sep. Purif. Technol., 192 (2018) 483-490.
[30] M. Peydayesh, T. Mohammadi, S.K. Nikouzad, A positively charged composite loose nanofiltration membrane for water purification from heavy metals, J. Membr. Sci., 611 (2020) 118205.
[31] Q. Song, Y. Lin, T. Ueda, Q. Shen, K.-R. Lee, T. Yoshioka, H. Matsuyama, A zwitterionic copolymer-interlayered ultrathin nanofilm with ridge-shaped structure for ultrapermeable nanofiltration, J. Membr. Sci., 657 (2022) 120679.
[32] C. Fang, S. Jeon, S. Rajabzadeh, L. Cheng, L. Fang, H. Matsuyama, Tailoring the surface pore size of hollow fiber membranes in the TIPS process, J. Mater. Chem., 6 (2018) 535-547.
[33] S.-Y. Wang, R.R. Gonzales, P. Zhang, T. Istirokhatun, R. Takagi, A. Motoyama, L.-F. Fang, H. Matsuyama, Surface charge control of poly(methyl methacrylate-co-dimethyl aminoethyl methacrylate)-based membrane for improved fouling resistance, Separation and Purification Technology, 279 (2021) 119778.
[34] S.-H. Park, Y. Ahn, M. Jang, H.-J. Kim, K.Y. Cho, S.S. Hwang, J.-H. Lee, K.-Y. Baek, Effects of methacrylate based amphiphilic block copolymer additives on ultra filtration PVDF membrane formation, Sep. Purif. Technol., 202 (2018) 34-44.
[35] Y.-F. Mi, G. Xu, Y.-S. Guo, B. Wu, Q.-F. An, Development of antifouling nanofiltration membrane with zwitterionic functionalized monomer for efficient dye/salt selective separation, J. Membr. Sci., 601 (2020) 117795.
[36] N.G.P. Chew, Y. Zhang, K. Goh, J.S. Ho, R. Xu, R. Wang, Hierarchically Structured Janus Membrane Surfaces for Enhanced Membrane Distillation Performance, ACS Appl Mater Interfaces, 11 (2019) 25524-25534.
[37] L. Zhang, L. Xu, H. Yu, P. Yao, M. Zhang, F. Guo, L. Yu, Capsaicin mimic-polyethyleneimine crosslinked antifouling loose nanofiltration membrane for effective dye/salt wastewater treatment, J. Membr. Sci., 641 (2022) 119923.
[38] H. Shi, L. Xue, A. Gao, Y. Fu, Q. Zhou, L. Zhu, Fouling-resistant and adhesion-resistant surface modification of dual layer PVDF hollow fiber membrane by dopamine and quaternary polyethyleneimine, J. Membr. Sci., 498 (2016) 39-47.
[39] J. Zhu, M. Tian, Y. Zhang, H. Zhang, J. Liu, Fabrication of a novel “loose” nanofiltration membrane by facile blending with Chitosan–Montmorillonite nanosheets for dyes purification, Chem. Eng. J., 265 (2015) 184-193.

[40] R. Nidhi Maalige, K. Aruchamy, A. Mahto, V. Sharma, D. Deepika, D. Mondal, S.K. Nataraj, Low operating pressure nanofiltration membrane with functionalized natural nanoclay as antifouling and flux promoting agent, Chem. Eng. J., 358 (2019) 821-830.

[41] J. Li, Z. Cui, R. Tao, S. Yang, M. Hu, C. Matindi, N.N. Gumbi, X. Ma, Y. Hu, K. Fang, J. Li, Tailoring polyethersulfone/quaternary ammonium polysulfone ultrafiltration membrane with positive charge for dye and salt selective separation, J. Polym. Sci., 58 (2020) 2603-2618.

[42] J. Wu, Z. Wang, Y. Wang, W. Yan, J. Wang, S. Wang, Polyvinylamine-grafted polyamide reverse osmosis membrane with improved antifouling property, J. Membr. Sci., 495 (2015) 1-13.

[43] Y.-H. Tong, Y.-Z. Wu, Z.-L. Xu, L.-H. Luo, S.-J. Xu, Photocatalytic self-cleaning EVAL membrane by incorporating bio-inspired functionalized MIL-101(Fe) for dye/salt separation, Chem. Eng. J., 444 (2022) 136507.

[44] Q. Chen, P. Yu, W. Huang, S. Yu, M. Liu, C. Gao, High-flux composite hollow fiber nanofiltration membranes fabricated through layer-by-layer deposition of oppositely charged crosslinked polyelectrolytes for dye removal, J. Membr. Sci., 492 (2015) 312-321.

[45] C. Wang, Y. Chen, K. Yang, X. Hu, Y. Zhang, Fabrication of tight GO/PVDF hollow fiber membranes with improved permeability for efficient fractionation of dyes and salts in textile wastewater, Polym. Bull., 79 (2021) 443-462.

Supporting Information

Development of loose nanofiltration PVDF hollow fiber membrane for dye/salt separation

Pengfei Zhang [a,b], Saeid Rajabzadeh [a,b,c], Qiangqiang Song [a,b], Ralph Rolly Gonzales [a], Yuandong Jia [a,b], Shang Xiang [a,b], Zhan Li [a], Hideto Matsuyama [a,b]*

[a] *Research Center for Membrane and Film Technology, Kobe University, 1-1 Rokkodaicho, Nada, Kobe 657-8501, Japan*

[b] *Department of Chemical Science and Engineering, Kobe University, 1-1 Rokkodaicho, Nada, Kobe, 657-8501, Japan*

[c] *School of Civil and Environmental Engineering, University of Technology Sydney (UTS), City Campus, Broadway, NSW 2007, Australia*

** Corresponding author: Professor H. Matsuyama*

E-mail address: matuyama@kobe-u.ac.jp (H. Matsuyama)

Tel. / Fax: +81 78 803 6180

Table S1. Summary of the spinning conditions for the PVDF/PSMA hollow fiber membranes

Preparation conditions	Parameters
Screw temperature (°C)	190
Dope solution: PVDF/GTA (wt%/wt%)	30/70
Dope solution extrusion flow rate (g min^{-1})	8.5
Copolymer solution: PSMA/SFL (wt%/wt%)	5/95
Copolymer solution extrusion flow rate (mL min^{-1})	4
Water quenching bath temperature (°C)	15
Bore liquid	GTA
Bore liquid flow rate (g min^{-1})	6.2
Air gap (cm)	25
Take-up speed (m min^{-1})	15

Table S2. Properties of dyes used in this study

Dye	Molecular structure	Molecular weight (g mol^{-1})	Charge	Max. absorption wavelength (nm)
Methyl blue (MB)	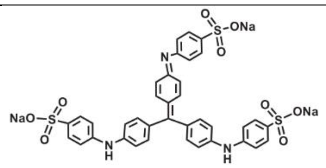	799.80	-3	626
Congo red (CR)	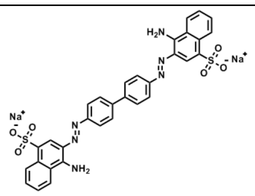	696.08	-2	495
Erythrosin B (EB)	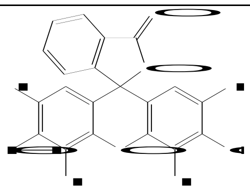	835.89	None	525
Janus Green B (JGB)	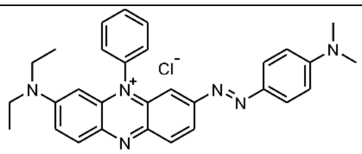	511.06	+1	660

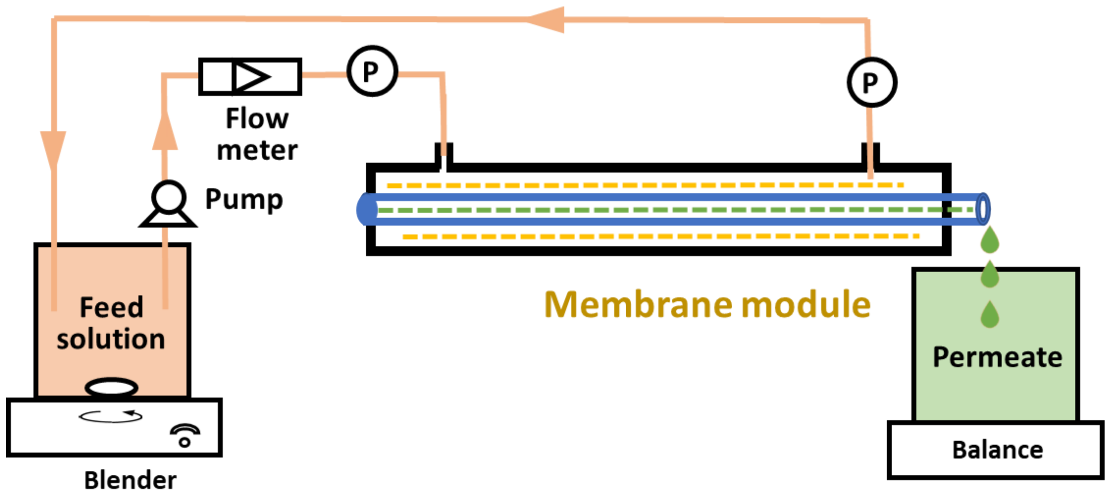

Fig. S1 Schematic description of cross-flow filtration test setup.

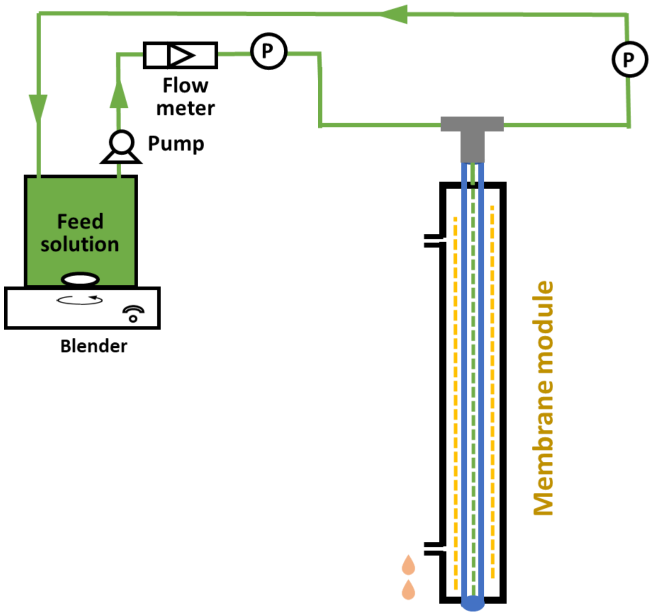

Fig. S2 Schematic description of backing washing process.

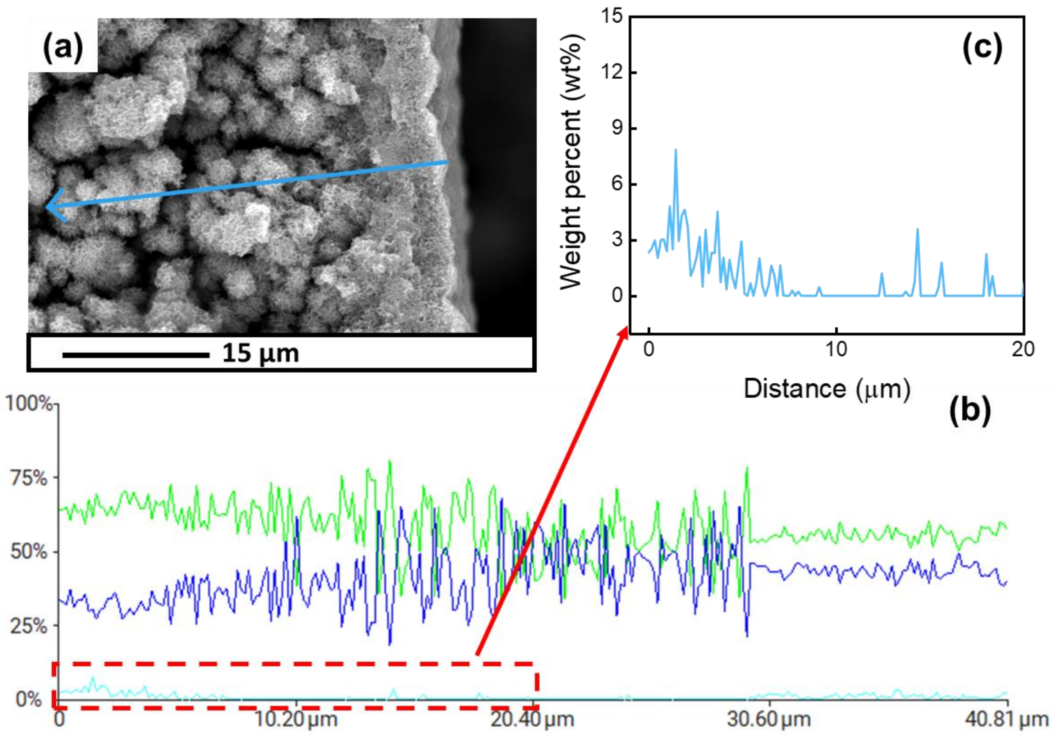

Fig. S3 Energy dispersive X-ray line scan. SEM image (a), elements composition by weight percent (b) and enlarged O element weight percent (c).

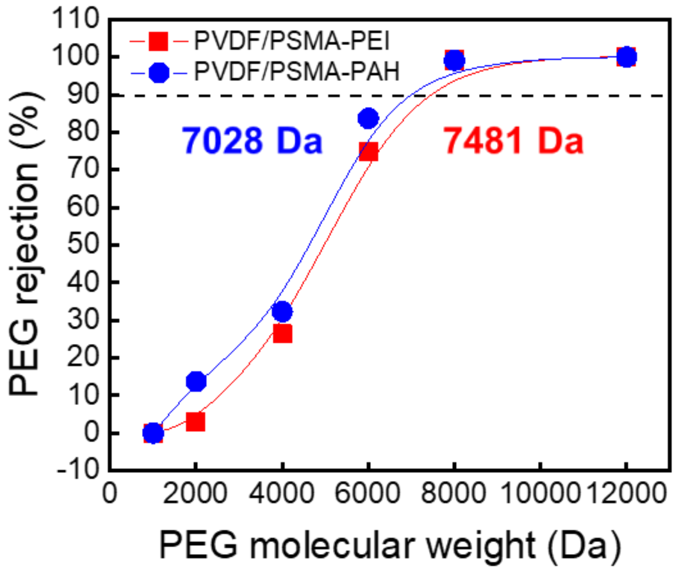

Fig. S4 PEG rejection of the PVDF/PSMA-PEI and PVDF/PSMA-PAH membranes.

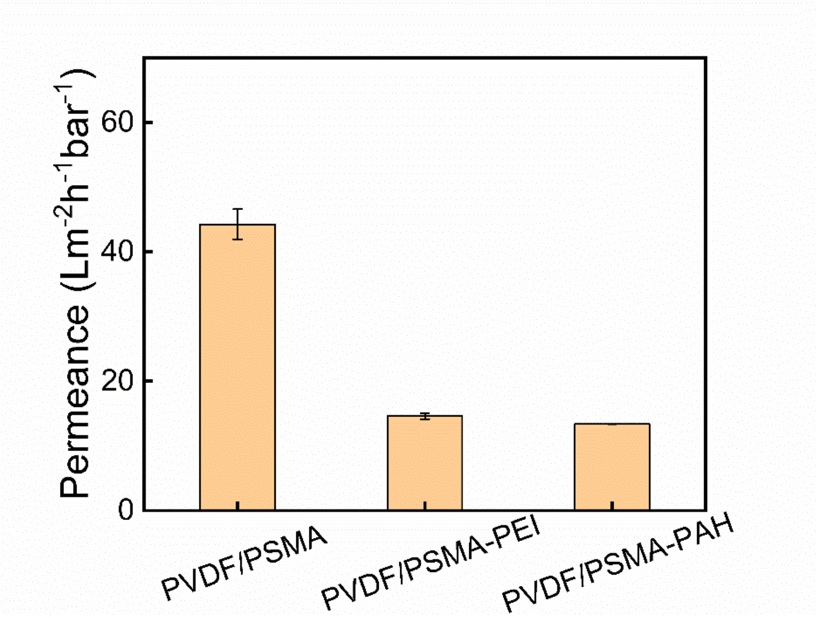

Fig. S5 Permeability in the case of feed CR aqueous solution at a pressure of 1 bar.